

Results and Discussion

Stability. Silver trifluoride is stable at room temperature in a dry atmosphere but is readily decomposed by atmospheric moisture. The products of this decomposition were identified as Ag_2O_2 and AgF from their X-ray powder patterns. The thermal stability study showed that AgF_3 starts to decompose at $163 \pm 1^\circ\text{C}$ under pumping. The weight change and the X-ray diffraction pattern of the residue indicated that it decomposes into AgF_2 and F_2 .

X-ray Data. The positions and intensities of the lines observed on the X-ray powder pattern of AgF_3 are listed in Table I. This pattern indicates a low symmetry of the lattice and could not be indexed. No similarities with other trifluorides were observed.

Vibrational Spectra. The infrared spectrum of AgF_3 was found to be quite distinct from that of AgF_2 . A strong broad band is observed at 600 cm^{-1} with two bands of medium intensity at 535 and 480 cm^{-1} . Superimposed on the fluorescence from the glass part of the spinning cell, the Raman spectrum of AgF_3 displays a strong line at 543 cm^{-1} and two lines of much weaker intensity at 573 and 261 cm^{-1} . Obviously no interpretation of these spectra is yet possible without other sources of structural information.

Chemical Properties. AgF_3 is not significantly soluble in HF or ClF_3 . Depending on the reaction conditions, it reacts at room temperature with liquid FNO to yield the new silver fluoro complexes NOAgF_3 and NOAgF_4 . The Ag^{2+} complex (Anal. Calcd for NOAgF_3 : Ag, 55.35; F, 29.25; N, 7.19; O, 8.21. Found: Ag, 55.55; F, 29.18; N, 7.15; O, 8.12 (by difference)) was obtained whenever the reactor contained any metallic parts (Monel, nickel, or stainless steel). The blue color of the excess of FNO recovered after the reaction indicated that nitrogen oxide had been formed, and this was confirmed by infrared analysis of a sample. The formation of NOAgF_3 is then easily explained by the reaction of AgF_3 and/or NOAgF_4 with these oxides. Only the use of an all-Teflon reactor together with fluorine added to FNO allowed the preparation of a pure sample of NOAgF_4 . Anal. Calcd for NOAgF_4 : Ag, 50.44; F, 35.53; N, 6.55; O, 7.48. Found: Ag, 50.70; F, 35.25; N, 6.27; O, 7.78 (by difference). Probably owing to the great reactivity and/or easy decomposition of this compound, its X-ray powder patterns always showed the presence of decomposition products, such as NOAgF_3 or AgF_2 , and not enough lines were available to fully characterize NOAgF_4 . On the other hand, the X-ray powder pattern of NOAgF_3 clearly indicated that this compound is isostructural with KAgF_3 .

Magnetic Properties. The measurements show that AgF_3 is paramagnetic and obeys the Curie-Weiss law in the temperature range studied (4-290 K). Three sets of measurements obtained on samples from different preparations gave a magnetic moment of $1.15 \pm 0.05 \mu_B$.

Owing to the great reactivity of AgF_3 and the eventual presence of degradation products, the origin of this paramagnetism has to be discussed. The X-ray powder patterns taken before and after the magnetic measurements did not show the presence of AgF_2 ; also, contrary to the findings for this compound,¹² no magnetic transition was observed for our sample. An uncontrolled hydrolysis also cannot account for the paramagnetism since the products of the hydrolysis, AgF and Ag_2O_2 (vide supra), are both diamagnetic.

On the other hand, the low value of the magnetic moment, when compared to the expected $2.83 \mu_B$ spin-only value for a $4d^8$ high-spin electronic configuration, deserves some comments. As stated above, no indication for an antiferromagnetic

behavior was noticed and no other lines other than those of AgF_3 were observed in the X-ray diffraction patterns. Therefore, neither an antiferromagnetic effect nor some crystalline impurity appears to account for the low value of the magnetic moment. Keeping in mind that the ion Pd^{2+} is isoelectronic with Ag^{3+} , it is interesting to mention the magnetic properties of palladium species. Whereas the difluoride is paramagnetic, only a few other Pd^{2+} fluoro derivatives are paramagnetic.¹³ The trifluoride was demonstrated^{3,14} to be the mixed-valency compound $\text{Pd}^{2+}[\text{PdF}_6]^{2-}$, and its paramagnetism was interpreted by the high-spin electronic configuration of Pd^{2+} ($d_{2g}^6 e_g^2$) and the low-spin configuration of Pd^{4+} ($d_{2g}^6 e_g^0$).

In a similar way, AgF_3 may be supposed to be the mixed-valency compound $\text{Ag}^{2+}[\text{AgF}_6]^{2-}$. With this formulation, the lower magnetic moment is obtained with a low-spin configuration of the ion Ag^{4+} corresponding to only one unpaired electron and the total magnetic moment of " AgF_3 " would be $1.73 \mu_B$ for the spin-only value. It is worth mentioning that a Jahn-Teller distortion is to be expected¹⁵ with ions of the electronic structure $t_{2g}^6 e_g^1$ in an octahedral site and that this would be compatible with the low symmetry of the lattice.

So far, attempts were unsuccessful to prepare other $\text{M}^{2+}[\text{AgF}_6]^{2-}$ salts (with M being a divalent element) that would be isomorphous with " AgF_3 ". Also, no single-crystal X-ray diffraction study of AgF_3 has so far been possible.

A second tentative explanation, which is less probable than the former one, is that there are Ag^{3+} ions in two different crystal sites, with only one of them leading to a paramagnetic ion. The spin-only value would then be equal to $2.83/2 \mu_B$ per AgF_3 entity.

Conclusions. The use of the strong fluorinating agent KrF_2 in HF solution has allowed us to obtain a new silver fluoride. This compound having the overall composition AgF_3 has been characterized. On the basis of its magnetic properties, AgF_3 might actually be $\text{Ag}^{2+}[\text{AgF}_6]^{2-}$, but this requires a confirmation by a crystal structure determination.

Acknowledgment. The authors thank Drs. P. Charpin and K. Christie for fruitful discussions.

Registry No. AgF_2 , 7783-95-1; KrF_2 , 13773-81-4; AgF_3 , 91899-63-7; FNO, 7789-25-5; NOAgF_3 , 91899-65-9; NOAgF_4 , 91899-67-1.

(13) Bartlett, N.; Maitland, R. *Acta Crystallogr.* **1958**, *11*, 747.

(14) Tressaud, A.; Wintenberg, M.; Bartlett, N.; Hagenmuller, P. C. R. *Hebd. Seances Acad. Sci., Ser. C* **1976**, *282*, 1069.

(15) Jolly, W. L. "Modern Inorganic Chemistry"; McGraw-Hill: New York, 1984; p 431.

Contribution from Ames Laboratory and the Department of Chemistry, Iowa State University, Ames, Iowa 50011

Kinetics and Mechanism of the Formation of Alkyl Radicals and Alkylpentaquo-chromium(2+) Complexes by the Reaction of Free Radicals Derived from (2-Hydroxy-2-propyl)pentaquo-chromium(2+) Ions with Alkyl Iodides

James H. Espenson,* Suzanne L. Bruhn, and Andreja Bakac

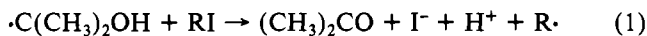
Received April 23, 1984

The unimolecular homolysis of organochromium cations¹⁻⁴ serves as a source of "stored" free radicals, which can be useful

(12) Charpin, P.; Dianoux, A. J.; Marquet-Ellis, H.; Nguyen-Nghi C. R. *Hebd. Seances Acad. Sci., Ser. C* **1967**, *264*, 1108.

(1) Kirker, G. W.; Bakac, A.; Espenson, J. H. *J. Am. Chem. Soc.* **1982**, *104*, 1249.

for determinations of reaction rates⁵⁻¹⁰ and for preparative chemistry. For the former use, one advantage this method offers over the generation and observation of R· directly is that special techniques (e.g., pulse radiolysis) are not needed. Also, it is applicable to slower reactions, for which pulse methods cannot readily be used. Moreover, radical self-reactions (dimerization and/or disproportionation) are avoided since [R·] remains very low throughout. We describe here the determination of k_{RI} for the reduction of several alkyl iodides by the $\cdot\text{C}(\text{CH}_3)_2\text{OH}$ radical (eq 1) and the identification of



the alkylchromium product. We also describe the preparation of CrR^{2+} on a larger scale in the case of $\text{R} = \text{CH}(\text{CH}_3)_2$, a complex previously prepared by other routes.^{11,12}

Experimental Section

Materials. Cyclopentyl and 2-propyl iodides were purified by shaking with aqueous sodium metabisulfite, followed by filtration through a Millipore-Q filter. Reagent grade methyl and ethyl iodides were used as received. Other reagents were prepared as before.⁵⁻¹⁰

Measurements. The reactions were monitored spectrophotometrically under strict anaerobic conditions by using syringe-septum techniques. The decrease in $[\text{CrC}(\text{CH}_3)_2\text{OH}^{2+}]$ was monitored at its 407-nm maximum ($\epsilon = 700 \text{ M}^{-1} \text{ cm}^{-1}$).¹³ The data followed pseudo-first-order kinetics, and the rate constant for each run was evaluated by the standard equations. The measurements were made at 25 °C in 0.100 M perchloric acid. The ionic strength was ca. 0.1 M, and ionic species other than H^+ and ClO_4^- were present at much lower concentrations. All of the reactions required use of 2-propanol as a cosolvent, since it is required for the in situ preparation of $\text{CrC}(\text{CH}_3)_2\text{OH}^{2+}$ from the reaction of Cr^{2+} and H_2O_2 .^{1-6,14} Much higher concentrations of 2-propanol than required for that purpose were used, in fact, to provide better solubility of the organic iodides. Some of the systems described here were studied at 3.0 M 2-PrOH, others at 10.0 M, and some at both.

Preparation of $\text{CrCH}(\text{CH}_3)_2^{2+}$. A solution containing 0.01 M hydrogen peroxide and 10.0 M 2-propanol was prepared in aqueous 0.13 M perchloric acid. The solution was cooled to 0 °C and deaerated by an active stream of Cr^{2+} -scrubbed nitrogen. A chromium(II) perchlorate solution and 2-propyl iodide were then injected to give $[\text{Cr}^{2+}] = 0.02 \text{ M}$ and $[(\text{CH}_3)_2\text{CHI}] = 0.20 \text{ M}$. Before ion-exchange separation, 50 mL of the solution was diluted with 150 mL of ice-cold water to lower [2-PrOH] to 2.5 M and $[\text{H}^+]$ to 0.03 M. The excess of unreacted iodide, which precipitated after the dilution, was filtered on a Millipore-Q filter pad. The solution was loaded onto a column of Sephadex C-25 resin cooled to 0 °C. The column was rinsed with 100 mL of 0.10 M perchloric acid, and then the desired complex was eluted with 0.25 M acid as a yellow-green band that was collected under N_2 in an ice-cooled receiving flask. The preparation yielded 25 mL of 6 mM $\text{CrCH}(\text{CH}_3)_2^{2+}$, ca. 30% of the theoretical yield.

Results

Acidolysis (eq 2) and homolysis (eq 3, a reversible reaction) take place concurrently. The latter produces $\cdot\text{C}(\text{CH}_3)_2\text{OH}$ radicals, which reduce alkyl iodides (eq 1) forming alkyl

Table I. Summary of Kinetic Data^a at 25.0 °C for Reactions of $\text{CrC}(\text{CH}_3)_2\text{OH}^{2+}$ in the Presence of Alkyl Iodides

rate const	3.0 M 2-PrOH	10.0 M 2-PrOH
k_A/s^{-1}	$(4.20 \pm 0.05) \times 10^{-3}$	$(6.19 \pm 0.02) \times 10^{-3}$
k_H/s^{-1}	$(1.27 \pm 0.03) \times 10^{-1}$	$(3.23 \pm 0.12) \times 10^{-1}$
$k_{RI}/\text{M}^{-1} \text{ s}^{-1}$		
CH ₃ I		$(6.0 \pm 0.5) \times 10^2$
CH ₃ CH ₂ I		$(1.70 \pm 0.08) \times 10^4$
(CH ₃) ₂ CHI	$(2.46 \pm 0.12) \times 10^5$	$(1.12 \pm 0.05) \times 10^5$
c-C ₅ H ₉ I	$(2.27 \pm 0.11) \times 10^5$	$(0.78 \pm 0.03) \times 10^5$

^a Determined in 0.1 M HClO_4 ($\mu = 0.1 \text{ M}$). Values are independent of $[\text{H}^+]$ in the range 0.01–1 M. The values of k_{Cr} from ref 13 used in eq 5 is assumed to be medium independent.

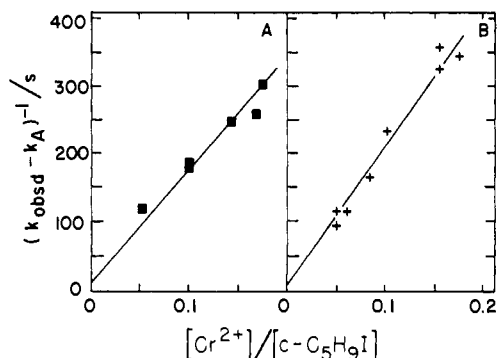
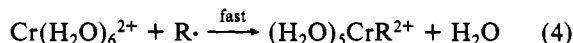
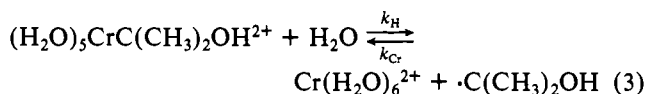
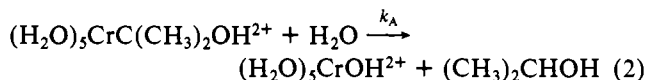
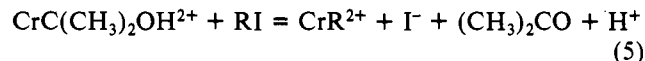


Figure 1. Plots of the kinetic data for the decomposition of $\text{CrC}(\text{CH}_3)_2\text{OH}^{2+}$ at 25.0 °C in the presence of cyclopentyl iodide according to eq 1. The straight lines correspond to the least-squares kinetic parameters (Table I). Values are shown at 2-propanol concentrations of (A) 3.0 M and (B) 10.0 M.

radicals. The latter react in turn very rapidly with Cr^{2+} to form CrR^{2+} (eq 4).



The overall stoichiometric reaction, for that portion proceeding along the free-radical route (eq 3 and 1 and 4), consists of the conversion of one organochromium cation to another:



The driving force lies (a) in the higher bond dissociation enthalpy and free energy of CrR^{2+} (e.g., $\text{Cr-c-C}_5\text{H}_9^{2+}$ has $\Delta H^\circ \sim 30$, $\Delta G^\circ = 16.7 \text{ kcal mol}^{-1}$, as compared to $\text{CrC}(\text{CH}_3)_2\text{OH}^{2+}$ with $\Delta H^\circ \sim 27$, $\Delta G^\circ = 11.7 \text{ kcal mol}^{-1}$) and (b) in the powerful reduction potential of $\cdot\text{C}(\text{CH}_3)_2\text{OH}$, $E^\circ \sim -1.2 \text{ V vs. NHE}$.¹⁵

Kinetics. The steady-state approximation is applicable to the free radicals, which are highly reactive and remain at concentrations so low that radical-radical reactions are unimportant. Since in the experiments both $[\text{Cr}^{2+}]$ and $[\text{RI}]$ are $\gg [\text{CrC}(\text{CH}_3)_2\text{OH}^{2+}]$, the reaction follows pseudo-first-order

- (2) Espenson, J. H. *Adv. Inorg. Bioinorg. React. Mech.* **1982**, *1*, 1.
- (3) Espenson, J. H. *Prog. Inorg. Chem.* **1983**, *30*, 189.
- (4) Mulac, W. A.; Cohen, H.; Meyerstein, D. *Inorg. Chem.* **1982**, *21*, 4106.
- (5) Espenson, J. H.; Shimura, M.; Bakac, A. *Inorg. Chem.* **1982**, *21*, 2537.
- (6) Shimura, M.; Espenson, J. H. *Inorg. Chem.* **1983**, *22*, 334.
- (7) McHatton, R. C.; Espenson, J. H. *Inorg. Chem.* **1983**, *22*, 784.
- (8) Chen, J.-T.; Espenson, J. H. *Inorg. Chem.* **1983**, *22*, 1651.
- (9) McHatton, R. C.; Espenson, J. H.; Bakac, A. *J. Am. Chem. Soc.* **1982**, *104*, 3531.
- (10) Muralidharan, S.; Espenson, J. H. *Inorg. Chem.* **1984**, *23*, 636.
- (11) Ryan, D. A.; Espenson, J. H. *J. Am. Chem. Soc.* **1982**, *104*, 704.
- (12) Espenson, J. H.; Connolly, P.; Meyerstein, D.; Cohen, H. *Inorg. Chem.* **1983**, *22*, 1009.
- (13) Cohen, H.; Meyerstein, D. *Inorg. Chem.* **1974**, *13*, 2434.
- (14) Bakac, A.; Espenson, J. H. *Inorg. Chem.* **1983**, *22*, 779.

- (15) Endicott, J. F. In "Concepts of Inorganic Chemistry"; Adamson, A. W., Fleischauer, P. D., Eds.; Wiley-Interscience: New York, 1975; pp 90–92.

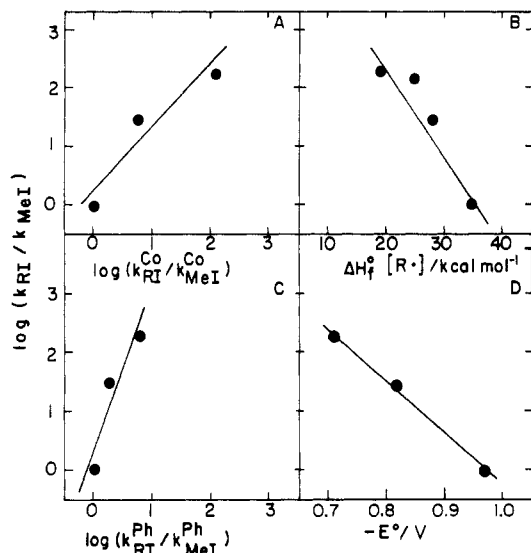


Figure 2. Attempted correlations of k_{RI} with parameters relating to the reductive dissociation of alkyl halides in terms of (A) $\log(k_{RI}^{Co}/k_{MeI}^{Co})$, where k^{Co} is the rate constant for $Co(CN)_5^{3-}$, (B) the enthalpy of formation of the alkyl radical, (C) $\log(k_{RI}^{Ph}/k_{MeI}^{Ph})$, where k^{Ph} is the rate constant for iodine atom abstraction by phenyl radicals, and (D) E^o (estd) for the electrochemical reduction of the alkyl iodide.

kinetics, $-d \ln [CrC(CH_3)_2OH^{2+}]/dt = k_{obsd}$, the expression for the experimental rate constant being

$$k_{obsd} = k_A + k_H k_{RI} [RI] / (k_{Cr} [Cr^{2+}] + k_{RI} [RI]) \quad (6)$$

The experimental data were analyzed by a nonlinear least-squares fit of the data to eq 6, with values of k_A and k_H set at values determined under these precise conditions (see Table I), and k_{Cr} taken to be $5.1 \times 10^7 M^{-1} s^{-1}$, the same as in 0.15–1.0 M 2-PrOH at $22 \pm 2^\circ C$.¹³ The resulting values of k_{RI} are given in Table I. Alternatively, the equation can be recast into a linear form (eq 7) that permits graphical representation of the data, as illustrated in Figure 1.

$$\frac{1}{k_{obsd} - k_A} = \frac{1}{k_H} + \frac{k_{Cr}}{k_H k_{RI}} \frac{[Cr^{2+}]}{[RI]} \quad (7)$$

Products. The identification of CrR^{2+} as the product provides evidence for the reactions given above. The 2-propyl complex was isolated by ion-exchange chromatography and identified by its absorption spectrum and by its reactions with Br_2 and Hg^{2+} . In the latter case, kinetic data were also used to confirm its identity. Other complexes ($CrCH_3^{2+}$, $CrCH_2CH_3^{2+}$) were identified by their visible/UV spectra and by the rates of their acidolysis reactions.

Interpretation and Discussion

The reactions shown are in complete accord with earlier studies of $CrC(CH_3)_2OH^{2+}$. They are supported in this case by the fit of the kinetic data to eq 6, as illustrated in Figure 1, and by the confirmation that CrR^{2+} is formed from a given RI.

The reaction between $\cdot C(CH_3)_2OH$ and RI is not without precedent, although the slowness of these reactions has precluded earlier kinetic measurements. For example, pulse-radiolysis experiments¹⁶ set $k < 10^5 M^{-1} s^{-1}$ for the reduction of CH_3I by $\cdot C(CH_3)_2OH$ at pH 7. In contrast, the conjugate base of the radical, a more powerful reducing agent, reacts readily (CH_3I , $k = 1.1 \times 10^8 M^{-1} s^{-1}$).¹⁶ The method employed here is applicable to less reactive substrates, which is the case with all of these alkyl iodides (Table I).

It is instructive to examine the factor(s) responsible for the changes in k_{RI} among the series of compounds examined. The variation of the rate constants with certain other kinetic and thermodynamic measures of the electron-transfer properties of alkyl iodides was explored. Each of the following gave approximate correlations: (a) the rates of inner-sphere reduction of RI by $Co(CN)_5^{3-}$ ¹⁷ (or for $Cr(15aneN_4)^{2+}$,¹⁸ which is not depicted but gives a quite comparable graph); (b) the enthalpy of formation of $R\cdot$;¹⁹ (c) the rate of iodine atom abstraction from RI by phenyl radicals;¹⁹ (d) the estimated standard reduction potentials of RI.²⁰ These correlations in a LFER sense are shown in Figure 2. Electron transfer from $\cdot C(CH_3)_2OH$ to RI appears to be governed by factors similar to those found for the several mechanisms (atom abstraction,²¹ electron transfer, dissociative reduction) by which RI is known to react. A finer distinction²² among the mechanisms cannot be made on the basis of the available data.

Acknowledgment. This work was supported by the U.S. Department of Energy, Office of Basic Energy Sciences, Chemical Sciences Division, under Contract W-7405-ENG-82.

Registry No. $(H_2O)_5CrCH(CH_3)_2^{2+}$, 60764-48-9; $(H_2O)_5CrC(CH_3)_2OH^{2+}$, 32108-93-3; CH_3I , 74-88-4; CH_3CH_2I , 75-03-6; $(C-H_3)_2CHI$, 75-30-9; $c-C_5H_9I$, 1556-18-9.

- (17) Halpern, J. *Ann. N.Y. Acad. Sci.* **1974**, *239*, 2.
- (18) Samuels, G. J.; Espenson, J. H. *Inorg. Chem.* **1979**, *18*, 2587.
- (19) Castelano, A. L.; Griller, D. *J. Am. Chem. Soc.* **1982**, *104*, 3655.
- (20) Ebersson, L. *Acta Chem. Scand., Ser. B* **1982**, *B36*, 533.
- (21) Halogen abstraction reactions by Et_3Si follow the reactivity order $CH_3X \geq C_2H_5X < i-C_3H_7X$; Chatgililoglu, C.; Ingold, K. U.; Scaiano, J. C. *J. Am. Chem. Soc.* **1982**, *104*, 5123. The absolute rate constants are, however, close to diffusion controlled in these systems, and the selectivity of the radical is diminished.
- (22) Kochi, J. K. "Organometallic Mechanisms and Catalysis"; Academic Press: New York, 1978; pp 138–168. A detailed discussion of these mechanisms is presented in this reference.

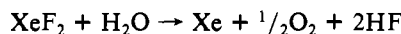
Contribution from the Chemistry Division,
Argonne National Laboratory, Argonne, Illinois 60439

Hydrolytic Reactions of Radon Fluorides

Lawrence Stein

Received May 1, 1984

The chemistry of radon has been studied by radioactive-tracer methods, since no stable isotopes of this element are known. It has been shown that radon reacts with fluorine,¹ halogen fluorides,² and a number of oxidizing salts.^{3,4} By comparing the properties of its products with known properties of krypton and xenon fluorides, it has been possible to deduce that radon forms a difluoride, RnF_2 , and derivatives of the difluoride, such as $RnF^+SbF_6^-$, $RnF^+TaF_6^-$, and $RnF^+BiF_6^-$. The trace products are reduced to elemental radon by water in reactions that are analogous to those of KrF_2 and XeF_2 with water:



(In contrast, XeF_4 and XeF_6 form stable solutions of XeO_3 .^{5,6})

- (1) Fields, P. R.; Stein, L.; Zirin, M. H. *J. Am. Chem. Soc.* **1962**, *84*, 4164.
- (2) Stein, L. *Science (Washington, D.C.)* **1970**, *168*, 362.
- (3) Stein, L. *Science (Washington, D.C.)* **1972**, *175*, 1463.
- (4) Stein, L. *Radiochim. Acta* **1983**, *32*, 163.
- (5) Malm, J. G.; Appelman, E. H. *At. Energy Rev.* **1967**, *7* (3), 3.
- (6) Bartlett, N.; Sladky, F. O. In "Comprehensive Inorganic Chemistry"; Trotman-Dickenson, A. F., Ed.; Pergamon Press: Oxford, 1973; Vol. 1, pp 213–330.

(16) Brault, D.; Neta, P. *J. Am. Chem. Soc.* **1981**, *103*, 2705.